http://dx.doi.org/10.5012/bkcs.2012.33.10.3258

Effects of Surface Nitrification on Thermal Conductivity of Modified Aluminum Oxide Nanofibers-Reinforced Epoxy Matrix Nanocomposites

Byung-Joo Kim, Kyong-Min Bae,† Kay-Hyeok An,* and Soo-Jin Park†,*

*Smart Composite Material Research Team, Carbon Valley R&D Division, Jeonju Institute of Machinery and Carbon Composites, Jeonju 561-844, Korea. *E-mail: khan@jmc.re.kr*
†Department of Chemistry, Inha University, Incheon 402-751, Korea
**E-mail: sjpark@inha.ac.kr*
Received May 7, 2012, Accepted July 10, 2012

Aluminum oxide (Al_2O_3) nanofibers were treated thermally under an ammonia (NH_3) gas stream balanced by nitrogen to form a thin aluminum nitride (AlN) layer on the nanofibers, resulting in the enhancement of thermal conductivity of Al_2O_3/epoxy nanocomposites. The micro-structural and morphological properties of the NH_3-assisted thermally-treated Al_2O_3 nanofibers were characterized by X-ray diffraction (XRD) and atomic force microscopy (AEM), respectively. The surface characteristics and pore structures were observed by X-ray photoelectron spectroscopy (XPS), Zeta-potential and N_2/77 K isothermal adsorptions. From the results, the formation of AlN on Al_2O_3 nanofibers was confirmed by XRD and XPS. The thermal conductivity (TC) of the modified Al_2O_3 nanofibers/epoxy composites increased with increasing treated temperatures. On the other hand, the severely treated Al_2O_3/epoxy composites showed a decrease in TC, resulting from a decrease in the probability of heat-transfer networks between the filler and matrix in this system due to the aggregation of nanofiber fillers.

Key Words : Aluminium oxide, Aluminum nitride, Thermal nitrification, Thermal conductivity

Introduction

Heat dissipation (or transfer) is a key issue in electric devices. Normally, polymeric insulating materials for electric devices require high thermal conductivity, low coefficient of thermal expansion, low dielectric constant *etc*..[1-9]

Many ceramic fillers, such as Al_2O_3,[2,6-8] SiO_2,[10,11] ZnO,[12,13] SiC,[14,15] AlN,[16,17] BN,[5,18] or graphene[3] are normally used as reinforcements in resins to enhance the thermal conductivity. These fillers can help build up the heat conducting networks in polymeric resins.

Zhou *et al.*[19] reported that the thermal conductivity of Al_2O_3/polymer composites can be enhanced by the particle sizes of the fillers, meaning that smaller fillers have higher conductivity. These behaviors suggest that smaller sized fillers can cause higher specific surface area of the fillers, resulting in a higher probability of heat transfer between the fillers and matrices. Other researchers attempted to use carbon nanotubes as an additive for high thermal conductivity of the polymer composites because the fibrous form of nanotubes can allow heat transfer (or dissipation).[1,4,6,8,15]

Among the ceramic fillers mentioned above, aluminum nitride (AlN) is a good filler for insulating resins due to the high thermal conductivity, low thermal expansion, and high electric resistivity.[16,17] On the other hand, the production of pure AlN nanofibers by chemical vapor decomposition (CVD) is difficult, and the final product is quite expensive.

Yang *et al.*[4] reported that core-shell hetero-structure nanowires or tubular nanowires can show different thermal conductivity according to the thickness ratio of each component due to phonon transport in cylindrical coordinates. This suggests that a very thin layer coating of AlN on Al_2O_3 can cause significant changes to the thermal conductivity of their composites.

Surface nitrification by various methods, such as a thermal method, plasma, *etc* makes it very simple to introduce nitrogen atoms into Al_2O_3 molecules, and finally form AlN layers partially on the Al_2O_3 or Al surfaces.[20-22] This method can help produce AlN-loaded Al_2O_3, which acts like pure AlN fillers.

In the present study, Al_2O_3 nanofibers were used as high thermal conductive fillers for epoxy matrix composites due to the fibrous form for heat transfer. The Al_2O_3 surface was converted partially to an AlN structure by a thermal nitrification method to enhance thermal conductivity of the epoxy composites dramatically. The effects of these treatments on surface and structural properties of modified Al_2O_3 nanofibers and their composites were observed.

Materials and Methods

Sample Preparation. The γ-Al_2O_3 nanofibers used in this study were purchased from Nano Technology Inc. (Average diameter is approximately 5-10 nm, and the aspect ratio is in the 50 to 200 range). Modified Al_2O_3 nanofibers were prepared as follows: (1) 1 g of nanofibers were dipped into ammonia water (10 wt %) for 30 min and dried at 100 °C for 12 h in a vacuum oven; (2) the dried nanofibers were heat-treated at 700-1100 °C (heating rate: 5 °C/min) for 2 h (holding time) with 1000 ppm of ammonia gas (feeding rate:

500 cm^3/g) balanced by nitrogen gas in a tubular furnace (quartz tube, diameter 100 mm, length 600 mm); and (3) they were then washed three times with distilled water and dried 100 °C for 12 h in a vacuum oven again.

The epoxy resins used in this study were DGEBA, supplied by Kukdo Chem. of Korea (YD-128), which had an epoxide equivalent weight (EEW) of 185-190 g/eq and a density of approximately 1.16 g/cm^3 at 25 °C. 4,4'-Diamino diphenyl methane (DDM) was used as a curing agent for the epoxy resins.

10 wt % of the modified Al_2O_3 nanofibers was suspended manually in an epoxy matrix, stirred for 30 min at 80 °C, and sonicated for 30 min to enhance the dispersion state of the nanofibers in the epoxy matrix. A curing agent was added to the mixtures at approximately 80 °C. The mixtures were degassed for 30 min in a vacuum oven, injected into a mold, and finally cured at 150 °C for 2 h.

Microstructures and Surface Morphologies. Wide-angle X-ray diffraction (XRD) of the modified Al_2O_3 nanofibers as a function of the treated temperatures was performed using a Rigaku Model D/MAX-III B diffraction meter equipped with a rotation anode using CuKα radiation (λ = 0.15418 nm).

The surface morphology of the modified Al_2O_3 nanofibers were examined by atomic force microscopy (AFM) using a XE-70 (Park Systems Co.) at room temperature under ambient pressure. In each case, an area of 1.0 × 1.0 μm was scanned in tapping mode.

Surface Characterizations. The surface functional groups on the modified Al_2O_3 nanofibers before and after treatment were examined by FT-IR (Bomen MB 102 FT-IR spectrometer, Hartmann & Brown Co.)

The zeta-potentials of the modified Al_2O_3 nanofibers were determined by electrophoretic mobility using an electrophoresis measurement apparatus, a Zeta-Potential & Particle Size Analyzer (ELS-Z, Otsuka Electronics, Japan) with a plate sample cell. The samples were dipped into distilled water and dispersed ultrasonically for 30 min, and measured under a −21.75 V/cm electric field and a −0.02 mA current at pH 7.

The XPS survey spectra of the modified Al_2O_3 nanofibers were collected using a MgKá X-ray source (1253.6 eV). The pressure inside the chamber was $< 5 \times 10^{-8}$ torr during analysis. The C_{1s} electron binding energy was referenced at 284.6 eV, and a curve-fitting procedure was carried out using a nonlinear least square curve-fitting program with a Gaussian-Lorentzian production function. For all elements, the atomic concentrations were estimated based on a comparison of the integrated peak intensities normalized by the atomic sensitivity factors.

Pore Structures. The N_2 isotherms were measured at 77 K using a BEL-Max (BEL Japan). The samples were outgassed at 573 K for 5-6 h to obtain a residual pressure of $< 10^{-3}$ torr. The amount of nitrogen adsorbed in the Al_2O_3 was used to calculate the specific surface area using the Brunauer-Emmett-Teller (BET) equation,[23] which has the following form:

$$\frac{1}{V(P_0/P)-1} = \frac{1}{V_m C_{BET}} + \frac{C_{BET}-1}{V_m C_{BET}} \frac{P}{P_0} \quad (1)$$

where P/P_0 is the relative pressure and C_{BET} is a BET constant, which is obtained by the intercept of the BET equation.

The total pore volume was estimated to be the liquid volume of nitrogen at a relative pressure of approximately 0.995, and the micropore volume was calculated using the *t*-plot method.[24]

The standard *t*-curve is expressed by the empirical de Boer equation:

$$t = \left(\frac{13.99}{\log P_0/P + 0.034} \right)^{\frac{1}{2}} \quad (2)$$

The calculation of *t* from the equation involves the assumption of hexagonal close packing, *i.e.* that the thickness of a single molecular layer of nitrogen is 3.54 Å.

The mesopore structures were analyzed using Barret-Joyner-Halenda (BJH) equations.[25]

$$RT \ln\left(\frac{P}{P_0}\right) = -2\sigma \frac{V_m}{r_k} \quad (3)$$

$$r_k = 4.14 \log\left(\frac{P}{P_0}\right) \quad (4)$$

$$r_{BJH} = r_k + t\left(\frac{P}{P_0}\right) \quad (5)$$

where r_k is the Kelvin radius, r_{BJH} is the pore radius from the BJH equation, V_m is the mole volume of the adsorbate, σ is the surface tension of the adsorbate, R is the gas constant, t is the *t*-thickness, and T is the adsorption temperature.

Thermal Conductivity. The thermal conductivity of the Al_2O_3 nanofibers/epoxy composites was evaluated using a quick thermal conductivity meter according to the hot wire method (QTM-500, Kyoto Electronis, Japan). When the electric power was applied to the heating wire, the temperature of the wire increased with time. The thermal conductivity can be calculated using the following equation:

$$\lambda = q \cdot \ln(t_2/t_1)/4\pi(T_2 - T_1) \quad (6)$$

where 'λ' refers to the thermal conductivity of the nanocomposites and '*q*' is the heat generated per unit length. '*T*' and '*t*' are the temperature and time, respectively[8]

Results and Discussion

Microstructures and Surface Morphologies. XRD and AFM were used to observe microstructure and morphology changes of Al_2O_3 nanofibers after thermal nitrification. Figure 1 shows XRD patterns of the Al_2O_3 nanofibers as a function of the NH_3-assisted treatment temperatures.

The as-received Al_2O_3 had characteristic peaks at 2θ = 14, 28, 46, and 68°, indicating Al_2O_3 structures. On the other hand, the peaks at 2θ = 14 and 28° disappeared after thermal

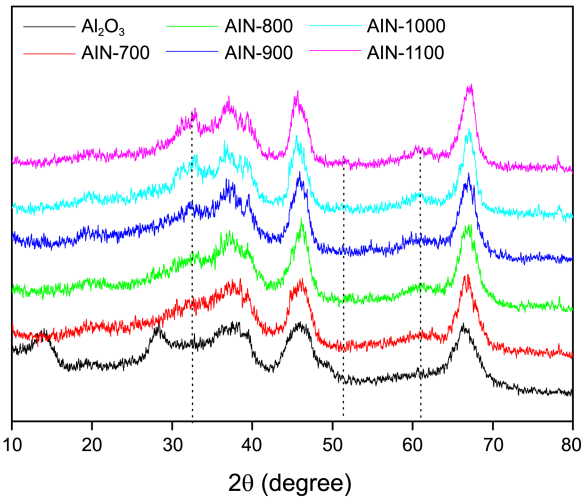

Figure 1. XRD patterns of the Al_2O_3 nanofibers as a function of the treatment temperatures.

nitrification. The peaks at 2θ = 46 and 68° were enhanced, and new peaks at 2θ = 32, 51, and 62° were formed in the modified Al_2O_3 nanofibers. This means that the microstructures of the Al_2O_3 nanofibers were changed. Kim *et al.*[22] reported that Al_2O_3 particles can be modified to AlN at high temperatures, and typical AlN characteristic peaks were observed at 2θ = 32, 36, 38, 51, 61, and 72°. In this same point of view, new AlN peaks were obtained in the thermally modified Al_2O_3 nanofibers, and that the original peaks of Al_2O_3 nanofibers were also enhanced (see peaks at 2θ = 45 and 67°). These behaviors suggest that AlN structures were introduced partially on the Al_2O_3 surfaces or formed very thin layers.[22,26,27]

Figure 2 shows AFM images of Al_2O_3 nanofibers as a function of the NH_3-assisted treatment temperature. The roughness of the as-received Al_2O_3 nanofibers was 2.95 nm but it increased with increasing treatment temperature. This suggests that the thermal treatments lead the aggregation of Al_2O_3 nanofibers, resulting in a very high roughness of 12.9 nm in the AlN-1100 sample.

Surface Characterization. Surface properties including surface chemical composition or surface functional groups before and after thermal nitrification were examined by FT-IR, Zeta-potential, and XPS.

Figure 3 shows FT-IR spectra of the Al_2O_3 nanofibers before and after the surface treatments. Typical Al_2O_3 peaks were observed at 1070 and 1640 cm^{-1} in the as-received sample. New peaks were noted at 750 and 850 cm^{-1} in the AlN-1100 sample, and the peak at 1640 cm^{-1} were decreased slightly. Kuchibhatla *et al.*[28] and Sanz-Hervás *et al.*[29] reported that various AlN peaks were observed at 600-850 cm^{-1} in the vapor grown AlN-coated SiO_2 samples. In this study, two peaks were noted at 755 and 825 cm^{-1}, indicating the formation of AlN molecules on Al_2O_3 nanofibers.

The changes in Zeta-potential can be evidence for the surface modification of Al_2O_3 nanofibers. Figure 4 shows the Zeta-potential of the Al_2O_3 nanofibers as a function of the NH_3-assisted treatment temperatures. The Zeta-potential

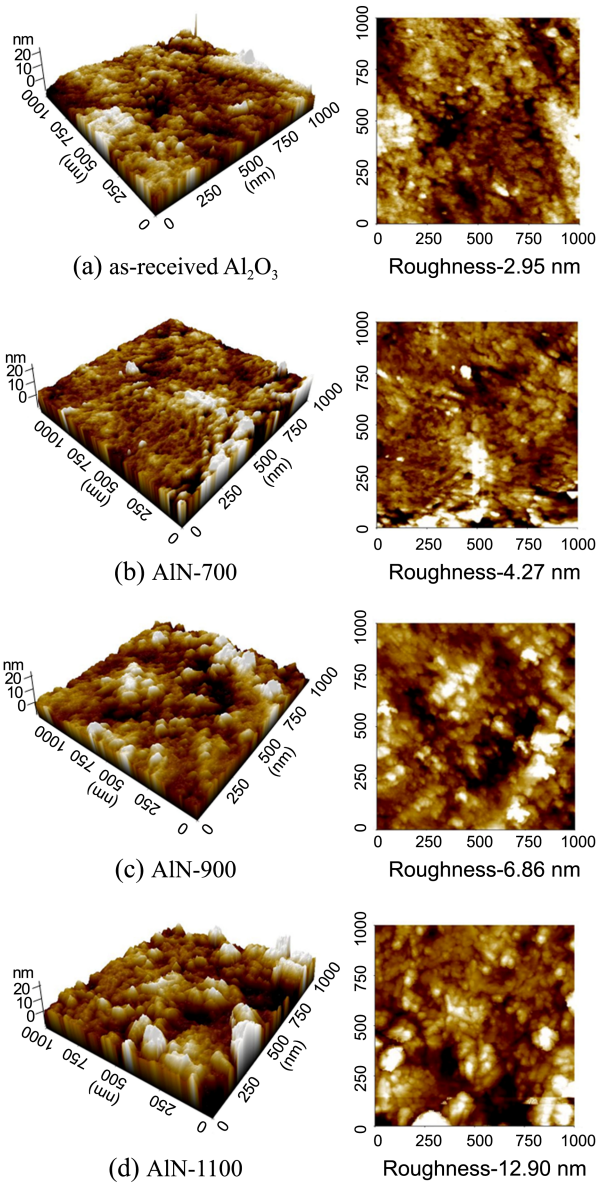

Figure 2. AFM images of the Al_2O_3 nanofibers as a function of the treatment temperatures.

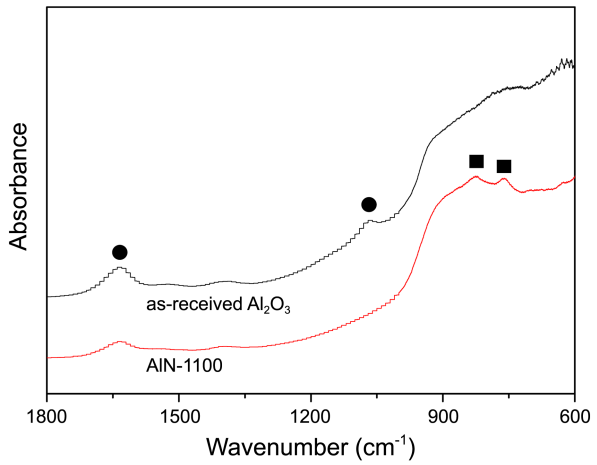

Figure 3. FTIR spectra of the Al_2O_3 nanofibers before and after the surface treatments.

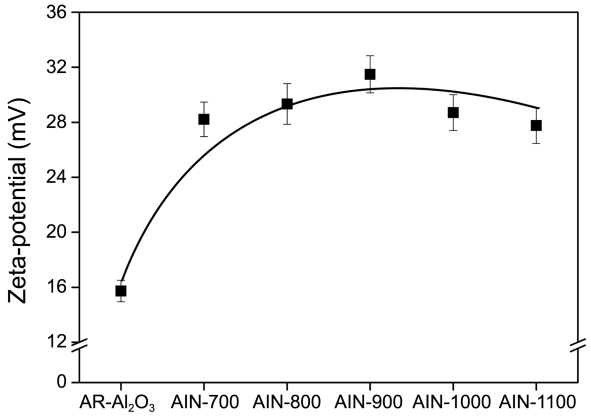

Figure 4. Zeta-potential of theAl_2O_3 nanofibers as a function of the treatment temperatures.

Table 1. Chemical Composition of Modified Al_2O_3 Nanofibers Before and After the NH_3-assisted Surface Treatments

Sample	O_{1s} (at.%)	Al_{2p} (at.%)	Al_{2p}/O_{1s}
As-received Al_2O_3	57.7	34.0	0.59
AlN-1100	53.9	33.4	0.62

of the as-received sample was 16 mV, and all modified samples showed higher values in the range of 26-31 mV. This suggests indicates that thermal nitrification can lead to high positive charges on the Al_2O_3 nanofibers due to the newly form AlN structure.[30]

XPS was used to confirm the changes in the surface functional groups on the Al_2O_3 nanofiber surfaces. The results are shown in Table 1 and Figures 5 and 6. They show the chemical composition, XPS survey spectra, and high resolution peaks of the Al_2O_3 nanofibers before and after thermal nitrification.

Table 1 lists the aluminum and oxygen content of the samples. The oxygen content of the AlN-1100 sample decreased after the thermal treatments. This suggests that some oxygen molecules might be replaced by nitrogen molecules, resulting in the formation of AlN structures on the Al_2O_3 nanofibers.

Figure 5 shows XPS survey spectra and high resolution peaks of the Al_2O_3 nanofibers before and after the surface treatments. In the high resolution peaks, the Al_{2p} were shifted slightly to higher binding energy region, but O_{1s} were shifted to a lower region. Figure 6 shows the XPS Sub-peaks of Al_{2p} and O_{1s} before and after surface treatments.

The Al_2O_3 nanofiber surfaces were composed of two functional groups, including metallic Al and Al-O. The specific ratio of the metallic Al was much higher than that of Al-O. In the case of AlN-1100, newly formed functional groups, the AlN peak were observed at 71 eV. As confirmed by XRD and FT-IR data, thermal nitrification by ammonia gas formed AlN on the Al_2O_3 surface. This means that some metallic Al or Al-O bond were modified and replaced with Al-N bonds. As shown in Figure 6(b), the specific ratio of metallic Al decreased in the AlN-1100 sample, indicating

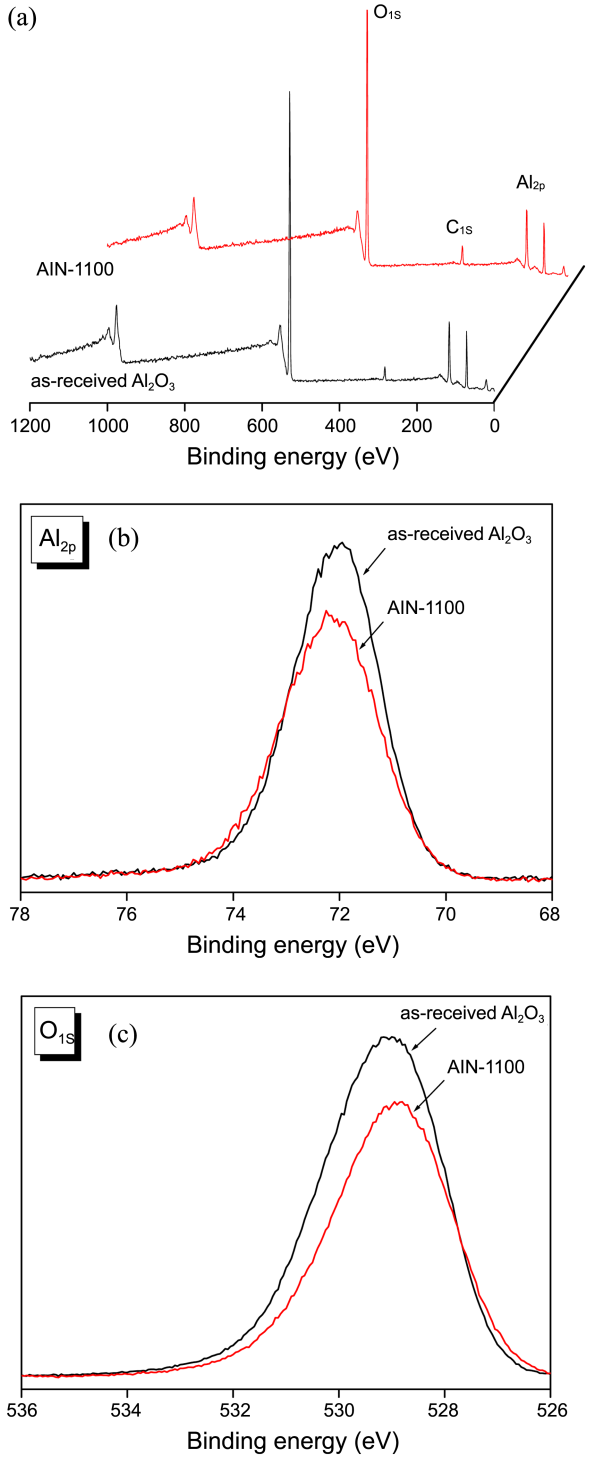

Figure 5. XPS survey spectra and high resolution peaks of the Al_2O_3 nanofibers before and after the surface treatments ((a) survey spectra, (b) high resolution Al_{2p}, (c) high resolution O_{1s}).

that metallic Al might be changed to Al-N in this work.

Figure 6(c) and (d) show the O_{1s} sub-peaks of Al_2O_3 nanofibers before and after thermal nitrification. The O_{1s} peaks were composed mainly of four characteristic Al_2O_3 peaks. The specific ratios of physisorbed H_2O and 'alpha' Al_2O_3 decreased after the thermal treatments. On the other hand, those of 'beta' and 'gamma' Al_2O_3 enhanced in the

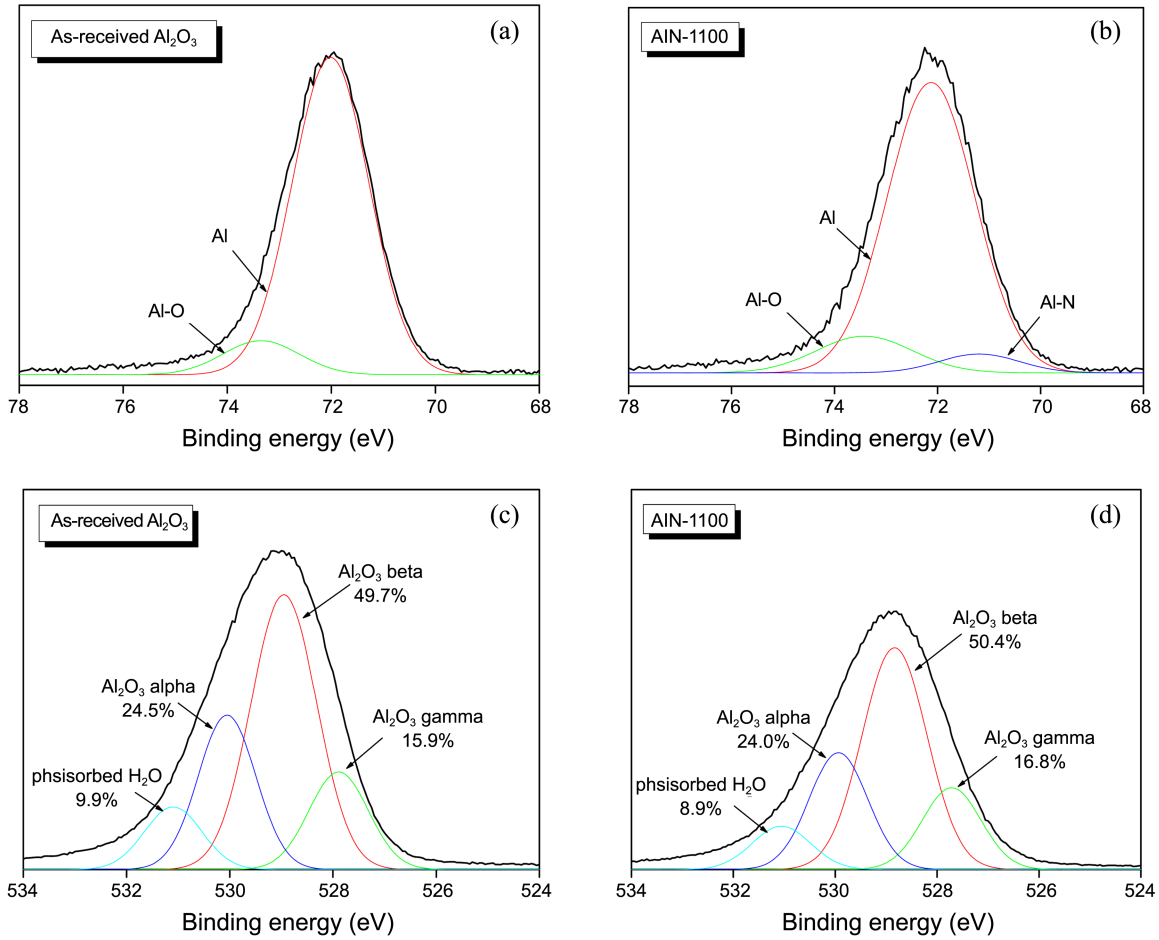

Figure 6. XPS sub-peaks of the Al_{2p} and O_{1s} peaks before and after the surface treatments ((a) Al_{2p} of as-received Al_2O_3, (b) Al_{2p} of AlN-1100, (c) O_{1s} of as-received Al_2O_3, (d) O_{1s} of AlN-1100).

AlN-1100 sample. As reported by reference,[31] the characteristic AlN peak was observed in the range of 528-527 eV. Therefore, in this study, the AlN peaks were probably summed with the peak of 'gamma' Al_2O_3 in Figure 6(d).

Pore Structures. Figure 7 shows the N_2/77 K adsorption isotherms of the Al_2O_3 nanofibers as a function of the NH_3-assisted treatment temperature.

The volume adsorbed decreased with increasing treatment temperature. As confirmed by AFM, all modified Al_2O_3 nanofibers aggregated with temperature, meaning that the textural properties including the total pore volume and specific surface area decreased. The logarithmic scale view shows that the decrease was proportional to the treated temperature.

Table 2 lists textural properties of the as-received and AlN-coated Al_2O_3 as a function of the nitrification temperature. The specific surface area of the as-received one was 305 m^2/g, which decreased to 126 m^2/g with temperature. The mean pore diameter showed a reverse trend with the specific surface area, meaning that micropores were severely blocked by the thermal treatments.[32-34]

Figure 8 shows the mesopore size distribution of the Al_2O_3 nanofibers as a function of the NH_3-assisted treatment temperatures calculated from the BJH equation. This shows that the mesopore volume also decreased with the treatment temperature.

These behaviors can lead a decrease in contact area between the fillers and matrix in the composite system due to the decrease in surface area, resulting in a disturbance of heat transfer from the fillers to the matrix (OR filler to filler due to the low dispersion in the matrix).[35]

Thermal Conductivity. Table 3 shows the thermal conductivity of the Al_2O_3 nanofibers as a function of the NH_3-assisted treatment temperatures. The thermal conductivity of the neat epoxy and as-received Al_2O_3 was 0.18 W/mK and 0.27 W/mK, respectively. In the case of the modified Al_2O_3 nanofibers-filled epoxy composites, the thermal conductivity was enhanced significantly except AlN-700. This suggests that thermal nitrification led the enhancement of thermal conductivity of the Al_2O_3 nanofibers/epoxy composites. On the other hand, the thermal conductivity increased to AlN-900 and then decreased, even though the AlN content showed the best in the AlN-1100 sample.

As listed in Table 2 and Figure 2, the specific surface area of the Al_2O_3 decreased with increasing treatment temperature, and the size of the nanofibers increased after the thermal treatments. This indicates that the modified Al_2O_3 nanofibers cannot be dispersed homogeneously in the epoxy

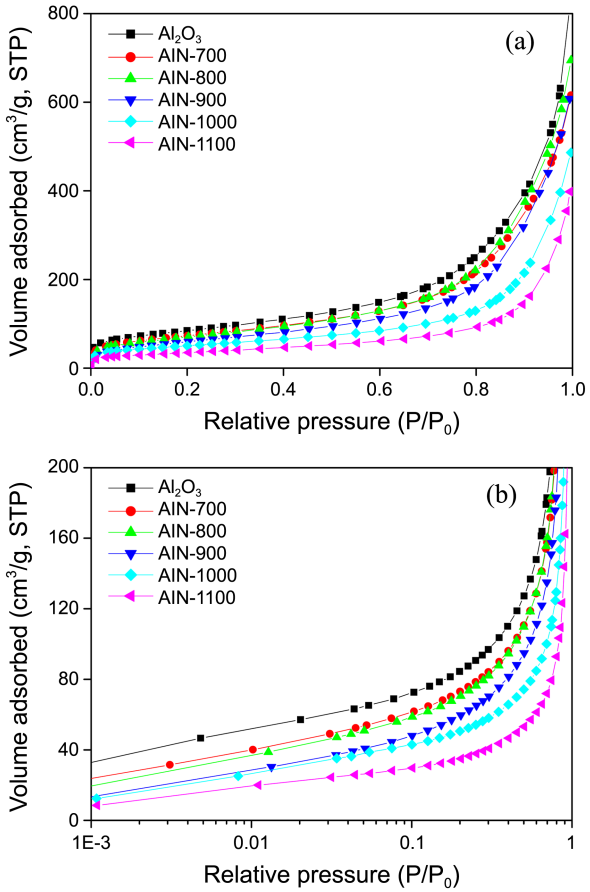

Figure 7. N_2/77 K isothermal curves of the Al_2O_3 nanofibers as a function of the treatment temperatures ((a) Decimal scale, (b) Logarithmic scale).

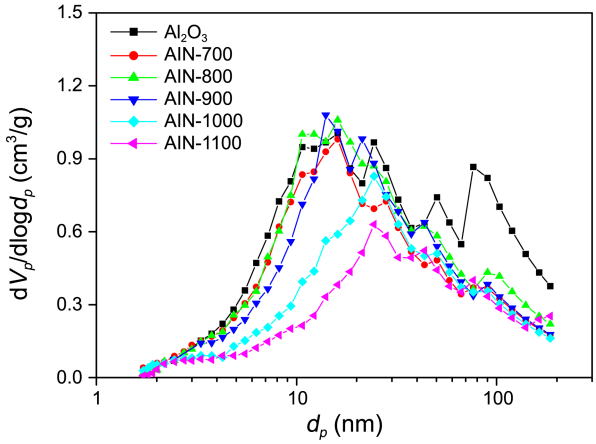

Figure 8. Pore size distribution of the Al_2O_3 nanofibers as a function of the treatment temperatures.

matrix compared to AlN-900 sample. Therefore, the heat transfer (or conduction) routes can be disturbed by the lack of dissipation probability between the fillers and matrix. Although the specific content of AlN-900 was not the best, the filler size and dispersion state were better than those of the AlN-1000 and 1100 samples, resulting in the highest of thermal conductivity in this work.

Figure 9 shows the cross-section images of each sample by a SEM analysis. Figure 7(a) shows relatively clean surface. In case of Al_2O_3/epoxy composites, the surface roughness increased due to the crack resistance by filler-resin interactions. Filler aggregation was observed in each Al_2O_3/epoxy sample. It was more severely occurred in AlN-1100/

Table 2. Textural Properties of the As-received and AlN-coated Al_2O_3 as a Function of the NH_3-assisted Treatment Temperatures

	as-received	AlN-700	AlN-800	AlN-900	AlN-1000	AlN-1100
S_{BET}[a] (m^2/g)	305	264	257	224	181	126
V_T[b] (cm^3/g)	1.20	0.91	1.01	0.91	0.71	0.57
d_p (nm)	13.94	14.69	15.74	16.28	17.25	18.07

[a]specific surface area (m^2/g) (P/P_0: 0.03-0.05) = $V_{ads} \times 6.02 \times 10^{23} \times 1.62 \times 10^{-19}$/22400. [b]total pore volume (cm^3/g) = V_{ads} (P/P_0 = 0.995) × (molar volume of liquid N_2/ molar volume of gaseous N_2)

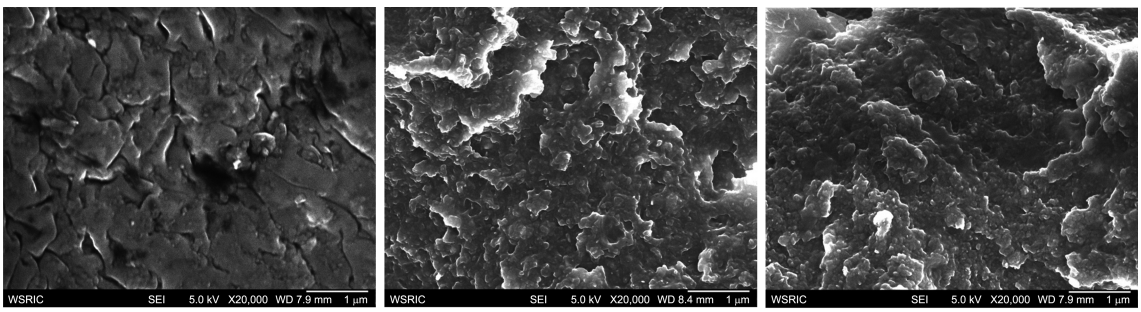

(a) (b) (c)

Figure 9. Cross-section images of each sample from SEM analysis; (a) Neat epoxy, (b) as-received Al_2O_3/epoxy, (c) AlN-1100/epoxy.

Table 3. Thermal Conductivity of Modified Al_2O_3 Nanofibers as a Function of the NH_3-assisted Treatment Temperatures

	Neat EP	AR-Al_2O_3	AlN-700	AlN-800	AlN-900	AlN-1000	AlN-1100
T.C. (W/mK)	0.18	0.27	0.27	0.29	0.34	0.35	0.33

epoxy sample, indicating that surface nitrification in this work caused filler aggregation as observed from AFM data, resulting in the high surface roughness of cross-section images and possibly low dispersion of fillers in the matrix.

Conclusions

The Al_2O_3 nanofibers were modified by thermal nitrification with ammonia gas at high temperatures. From the X-ray studies, the formation of AlN structures on the Al_2O_3 surface were confirmed, and the specific content increased with increasing NH_3-assisted treatment temperature. On the other hand, the surface areas of the AlN/Al_2O_3 nanofibers decreased despite the increase in AlN content. In conclusion, the AlN-900/epoxy sample showed the best thermal conductivity due to the suitable AlN content and good dispersion of fillers in the matrix.

Acknowledgments. This research was supported by a grant from the Fundamental R&D Program for Technology of World Premier Materials funded by the Ministry of Knowledge Economy, Republic of Korea.

References

1. Shen, S.; Henry, A.; Tong, J.; Zheng, R.; Chen, G. *Nature Nanotechnol.* **2010**, *5*, 251.
2. Rolinski, E. J.; Sweeney, T. L. *J. Chem. Eng. Data* **1968**, *13*, 203.
3. Balandin, A. A.; Ghosh, S.; Bao, W.; Calizo, I.; Teweldebrhan, D. *Nano Lett.* **2008**, *8*, 902.
4. Yang, R.; Chen, G.; Dresselhaus, M. S. *Nano Lett.* **2005**, *5*, 1111.
5. Terao, T.; Zhi, C.; Bando, Y.; Mitome, M.; Tang, C.; Golberg, D. *J. Phys. Chem. C* **2010**, *114*, 4340.
6. Sanada, K.; Tada, Y.; Shindo, Y. *Compos. A* **2009**, *40*, 724.
7. Fu, J. F.; Shi, L. Y.; Zhong, Q. D.; Chen, Y.; Chen, L. Y. *Polym. Adv. Technol.* **2011**, *22*, 1032.
8. Hong, J. H.; Lee, J.; Jung, D.; Shim, S. E. *Thermochim. Acta* **2011**, *512*, 34.
9. Garrett, K. W.; Rosenberg, H. M. *J. Phys. D* **1974**, *7*, 1247.
10. Kistler, S. S.; Caldwell, A. G. *Ind. Eng. Chem.* **1934**, *26*, 658.
11. Cui, W.; Du, F.; Zhao, J.; Zhang, W.; Yang, Y.; Xie, X.; Mai, Y. W. *Carbon* **2011**, *49*, 495.
12. Singh, A. K. *Adv. Powder Technol.* **2010**, *21*, 609.
13. Lim, W.; Craciun, V.; Siebein, K.; Gila, B. P.; Norton, D. P.; Pearton, S. J.; Ren, F. *Appl. Surf. Sci.* **2008**, *254*, 2396.
14. Popovska, N.; Alkhateeb, E.; Fröba, A. P.; Leipertz, A. *Ceram. Int.* **2010**, *36*, 2203.
15. Hong, J.; Choi, H. S.; Lee, K. S.; Shim, S. E. *Polym. Int.* **2012**, *61*, 639.
16. Zhou, W. *Thermochim. Acta* **2011**, *512*, 183.
17. Jung, W. S. *Bull. Korean Chem. Soc.* **2009**, *30*, 1563.
18. Tang, C.; Bando, Y.; Liu, C.; Fan, S.; Zhang, J.; Ding, X.; Golberg, D. *J. Phys. Chem. B* **2006**, *110*, 10354.
19. Zhou, W.; Qi, S.; Tu, C.; Zhao, H.; Wang, C.; Kou, J. *J. Appl. Polym. Sci.* **2007**, *104*, 1312.
20. Tan, B. J.; Xiao, Y.; Suib, S. L. *Chem. Mater.* **1992**, *4*, 648.
21. Oh, S. M.; Park, D. W. *Thin Solid Films* **1998**, *316*, 189.
22. Kim, J. K.; Jung, W. S. *J. Ceram. Soc. Japan* **2011**, *119*, 351.
23. Brunauer, S.; Emmett, P. H.; Teller, E. *J. Am. Chem. Soc.* **1938**, *60*, 309.
24. Lippens, B. C.; de Boer, J. H. *J. Catal.* **1965**, *4*, 319.
25. Do, D. D. *Adsorption Analysis: Equilibria and Kinetics*; Imperial College Press: London, 1998.
26. Gálvez, M. E.; Hischier, I.; Frei, A.; Steinfeld, A. *Ind. Eng. Chem. Res.* **2008**, *47*, 2231.
27. Gálvez, M. E.; Frei, A.; Halmann, M.; Steinfeld, A. *Ind. Eng. Chem. Res.* **2007**, *46*, 2047.
28. Kuchibhatla, S.; Rodak, L. E.; Korakakis, D. *Thin Solid Films* **2010**, *519*, 117.
29. Sanz-Hervás, A.; Iborra, E.; Clement, M.; Sangrador, J.; Aguilar, M. *Diam. Relat. Mater.* **2003**, *12*, 1186.
30. Park, J. S.; Lee, H. J.; Choi, S. J.; Geckeler, K. E.; Cho, J.; Moon, S. H. *J. Colloid Interface Sci.* **2003**, *259*, 293.
31. Liao, H. M.; Sodhi, R. N. S.; Coyle, T. W. *J. Vac. Sci. Technol. A* **1993**, *11*, 2681.
32. Kim, B. J.; Park, S. J. *J. Colloid Interface Sci.* **2010**, *342*, 575.
33. Kim, B. J.; Park, S. J. *Int. J. Hydrogen Energy* **2011**, *36*, 648.
34. Kim, Y. Y.; Yun, J.; Lee, Y. S.; Kim, H. I. *Carbon Lett.* **2011**, *12*, 48.
35. Heo, G. Y.; Seo, M. K.; Oh, S. Y.; Choi, K. E.; Park, S. J. *Carbon Lett.* **2011**, *12*, 53.